Review Paper

Ion Exchange Membranes for Reverse Electrodialysis (RED) Applications - Recent Developments

Mine Eti [1], Nur Hidayati Othman [2], Enver Güler [3,*], Nalan Kabay [1,*]

[1] Ege University, Department of Chemical Engineering, 35100 Izmir, Turkey
[2] School of Chemical Engineering, College of Engineering, Universiti Teknologi MARA, Shah Alam, 40450 Selangor Darul Ehsan, Malaysia
[3] Atılım University, Department of Chemical Engineering, 06830 Ankara, Turkey

## Article info

Keywords

Graphical abstract

Highlights

- RED is capable of producing power based on salinity gradient.
- Ion exchange membranes are the key components affecting the performance of RED.
- Nanocomposite and pore filling membranes exhibit high performances in RED.

Abstract

The innovative membrane-based technology called reverse electrodialysis (RED) is capable of producing electrical power from the controlled mixing of two aqueous streams of different salinity. There has been tremendous progress so far in the development of RED process in terms of system development, spacer design, membranes properties and operational conditions optimization. Among those, characteristics of the ion exchange membranes are found to be the critical element affecting the performances of RED process. In this respect, a brief overview of the latest developments in ion exchange membranes were presented in this review, focussing on their properties and performances in RED applications. The recent developments of nanocomposite and ion selective membranes, particularly pore filling ion exchange membranes due to their high performances and inexpensive fabrication cost were also summarized. Shortly, fouling problem for the ion exchange membranes employed in the RED system was mentioned.
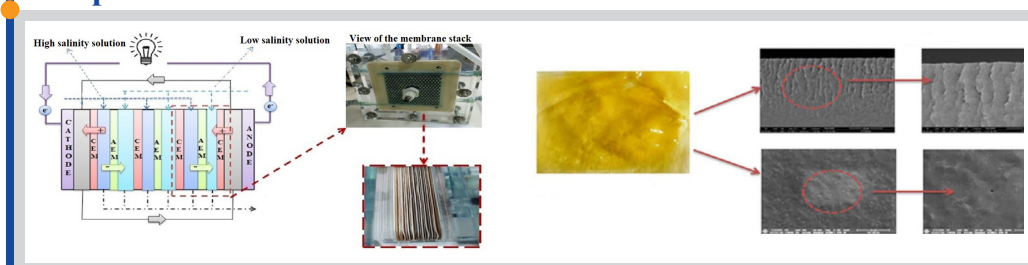
Contents

1. Introduction

It has a vital importance to use renewable energy today for reducing the fossil energy consumption rate thus air pollution and carbon dioxide emission. In recent years, the development of technologies that generate renewable energy from solar, wind and geothermal sources has attracted considerable attention. In addition to such sources, salinity gradient, a novel form of sustainable energy obtained by combining two different types of water with variable salinities, is considered to have a great potential [1]. The calculated amount of salinity gradient energy is estimated to be in the range of 1.4-2.6 TW [2]. This amount is more than the total global energy needed.

Pressure-retarded osmosis (PRO) and RED are two membrane-based techniques that are capable to convert blue energy into electricity [3]. Due to the increased power density and higher energy recovery, PRO appears to be more suitable for power generation from highly concentrated brines. PRO is based on water transport through semi-permeable membranes, where the driving force to generate energy for PRO is the pressure difference. On the other hand, RED appears to be more favorable for power generation by mixing seawater and river water. RED harvests the change in Gibbs free energy when waters with different salinities are mixed. Another reason of

choice between RED and PRO in certain situations is that RED is less prone to fouling than PRO because in RED process, only ions move through the hydrophilic membranes in RED while water permeation is the case in PRO when osmotic pressure gradient is utilized [4-7].

The RED system has the similar design of the conventional electrodialysis (ED) system. The only difference is that while the feed solutions with the similar compositions are pumped to each compartment in the ED system, two feed solutions having different salinities are fed to the RED system. The driving force in the ED process is electrical potential, while the salt concentration difference in the RED process to generate electrical power [8].

The essential parts of a laboratory scale RED membrane stack and its view are depicted in Figure 1. The membrane stack consists of a successive arrangement of certain numbers of ion exchange membranes (IEMs), known as cation exchange membranes (CEMs) and anion exchange membranes (AEMs) placed between electrodes, forming cell pairs. The salinity gradient on both sides of a membrane allows ions to pass through in opposite directions as shown in Figure 2. The ionic mobility creates a potential difference in the cell pair. As the number of cell pairs increases, it is possible to create a significant amount of potential difference. This potential difference activates the redox reactions in the electrodes. The redox pairs used in the electrode compartment have an important role in the RED system as they convert the ionic current into the electrical current. The electrode solution is constantly circulated between anode and cathode. By providing an external circuit between anode and cathode, an electrical current is created by the electron transport. This current then generates the electrical power [9,10].

A membrane connects or divides two contiguous stages and let substances between phases be transferred [11]. These boundaries are referred to as ion exchange membranes (IEMs) when they include functional groups. IEMs are classified into two types as CEMs and AEMs.

While cations are allowed to move towards the CEMs, anions cannot pass through the CEMs due to their negative charges. In AEMs, because the fixed charges in the polymer matrix are positive, anions are transported through the AEMs while cations cannot pass through this membrane. This principle was first explained by the Donnan exclusion [1].

In RED stacks, there are some system related limitations. Spacer materials and geometry are important factor for the stacks. Spacers are frequently required to assist IEMs, create flow channels, and facilitate mixing. Increased mixing has been shown to reduce concentration polarization. The thickness of the spacer undeviatingly influences the electrical resistance of the low salinity compartment, so it has a significant effect on the power output [19]. Dlugolecki et al. [21] studied spacer shadow effect by using commercial Neosepta AMX, Neosepta CMX membranes and spacers with the thicknesses of 0.2 mm and 0.5 mm at different flow rates ranged between 0.06 and 1.1 cm/s. They demonstrated that concentration polarization occurs at low linear flow rates and it may be greatly reduced by raising the solution flow rate and decreasing the spacer thickness. They observed that stack resistance increased when 0.2 mm spacer was used.

In ED and RED applications, each process should have its own optimized cell design. For example, the spacers used in ED units are thicker than the spacers used in RED units to minimize the electrical resistance and increase the power output [8]. Currently, commercial ion exchange membranes have been developed mainly for ED applications. However, ion exchange membranes in the RED system should have some specific properties such as high selective-permeability, low electrical resistance, high mechanical strength, acceptable chemical stability and low cost [11,12]. The existing ion exchange membranes contain a reinforcing filler material to provide mechanical strength and therefore, they are generally thick in ED applications. Thus, the existing ion exchange membranes need to be redesigned for RED applications.

The PFMs contain porous substrate and ion exchange polymer filled in the pores that can exhibit high ionic conductivity and high mechanical strength. Importantly, the strong porous substrate effectively inhibits IEMs from swelling excessively. Additionally, they might be manufactured in a more cost-effective manner, such as a continuous roll-to-roll process [62].

Production of PFMs with a relatively thin (<100 μm) film thickness can be a good alternative for RED systems. These membranes are formed by filling a fine-porous support material within polymer electrolyte structures [13-15]. Thus, the membrane synthesis of a desired thickness is possible by controlling the thickness of the porous support material.

Polymerization-chloromethylation-amination steps are required to prepare the AEMs [16,17]. Chloromethylation reaction is a process that should be avoided during membrane synthesis due to the release of some toxic chemicals. Using polymers that have inherent chloromethyl groups is a good solution to overcome this problem [17]. The best example of such polymers is polyepichlorohydrin polymer, a thermoplastic material that is cheap and easily synthesized [17]. These materials can increase the

mechanical strength of the supporting inert polymers when they are added to the membrane structure because they have high elastic properties. It is possible to make a homogeneous mixture using polymers such as polyacrylonitrile dissolved in the same solvent.

Another way to enhance the mechanical strength is to crosslink the polymer chains and provide a reticulated network structure. The use of diamine crosslinkers (eg DABCO-1,4-diazobicyclo [2.2.2] octane) provides a significant advantage in the preparation of AEMs in one step to provide both cross-linking and ion exchange characters to the IEMs [1]. It is possible to obtain clear solution when blending inert polymers, such as polyacrylonitrile, to the casting solution resulting in a homogenous mixture for membrane peparation by solvent evaporation.
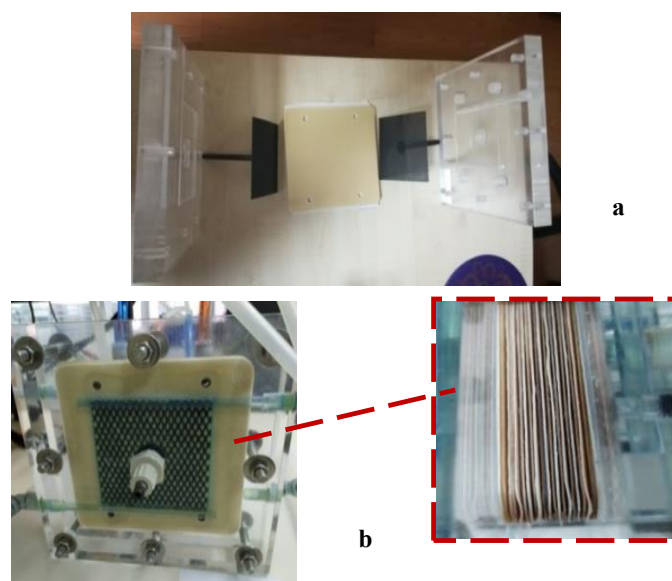

Fig. 1. a) Essential parts of laboratory scale RED stack, b) side view of the stack and IEMs.
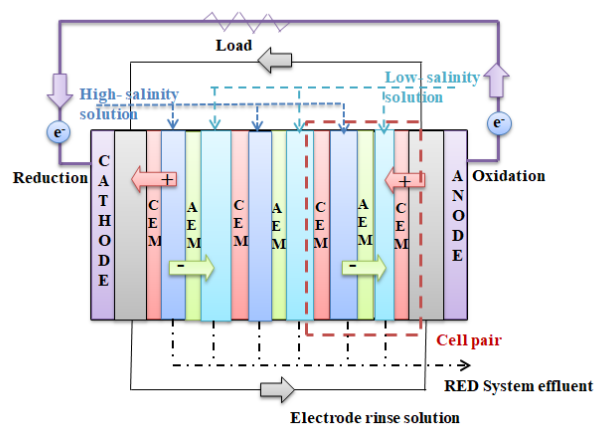

Fig. 2. Schematic of an RED system.

2. Properties of IEMs

Permselectivity and electrical resistance of IEMs are two crucial parameters for their performances in the RED system. Changes in these two parameters affect water content, ion exchange capacity, and fixed charge density of IEMs. For the structural stability and ionic transport characteristics, water content is of fundamental relevance. There is a relation between the ionic resistance and permselectivity of AEMs, because polymers having higher degree of swelling have lower ionic resistance and lower

permselectivity [7, 18].

Degree of swelling (DS) can be found using Equation 1 [7]:

$$DS = \frac{m_{wet} - m_{dry}}{m_{dry}} x100 \tag{1}$$

In this equation, m_{wet} and m_{dry} are the wet and dry weights of the membrane, respectively.

Ion exchange capacity (IEC) represents the amount of the charged groups in the IEMs. It is expressed as the milliequivalents (meq) of charged groups contained in g amount of dry membrane [7,19] and can be calculated by using Equation 2 [7]:

$$IEC = \frac{V_{AgNO_3}}{w_{dry}} x C_{AgNO_3} \tag{2}$$

in this equation, V_{AgNO3} indicates the volume (mL) of AgNO$_3$ solution consumed in a titration at the equivalence point, w_{dry}, dry membrane weight (g), and C_{AgNO3} indicates the concentration (mg/L), of AgNO$_3$ solution used.

The ion transport of the membranes depends on the swelling degree and the type and amount of charged functional groups attached to polymer backbone. This parameter, defined as the fixed charge density, is preferred to be as high as possible. Fixed charge density (C_{fix}), is expressed as the IEC per unit swelling (mmol constant charge groups per g-membrane), and it is calculated by dividing the IEC by the degree of swelling, which is shown in Equation 3 [7]:

$$C_{fix} = \frac{IEC}{SD} \tag{3}$$

Permselectivity and electrical resistance are two crucial features that increase the efficiency of the RED system [19,20]. The co-ions should be entirely omitted from the membrane process to achieve a completely permselective membrane and permselectivity of ions is related to the Donnan exclusion [11].

Permselectivity means that IEMs may preferentially carry counter-ions (e.g. CEM cations) and rule out co-ions (e.g. CEM anions). Theoretically, perfect ion exchange membranes have permselectivity of 1; but in practice, permselectivity value is less than 1 because transport of co-ions are unavoidable [19]. The permselectivity is commonly determined by dividing the calculated electrical potential difference by the theoretical value that should apply if the membrane is ideal, which is shown in Equation 4 [19]:

$$Permselectivity = \frac{E_{meas}}{E_{theo}} * 100 \tag{4}$$

Membrane resistance can be explained as the impediment of the passage of ionic current through the polymer matrix. If membrane resistance is higher in the RED stack, voltage decreases and power output will be reduced [21]. Resistance measurement can be done by direct current (DC) or alternative current (AC) methods. For the DC method, chronopotentiometry is used while electrochemical impedance spectroscopy method is used in the AC method [18,19]. IEMs with high IEC and high SD typically have a poor area resistance and limited permselectivity [19].

Potentiostat device is used for the measurement of power density and open circuit voltage (OCV) values with the method of multiple step chronopotentiometry. OCV can be defined as the potential difference caused by the salinity gradient defined by the Nernst equation which is calculated from Equation 5.

$$E_{OCV} = N \frac{2\alpha RT}{zF} \ln\left(\frac{a_c}{a_d}\right) \tag{5}$$

in this equation, α is the average permselectivity of a membrane pair (dimensionless), N is the number of membrane cells (dimensionless), R is the gas constant (8.314 J/mol K), T is the absolute temperature (K), z is the electrochemical valence, F is the Faraday constant (96,485 Cmol^{-1}), a_c is the activity of the concentrated salt solution (mol L^{-1}) and a_d is the activity of the diluted salt solution (mol.L^{-1}).

Stack resistance is related with the AEM (R_{aem}) and CEM (R_{cem}) resistances and the electrode resistance and the thickness of the membranes and also inversely proportional with the conductivity of the diluted and concentrated salt water compartments (Equation 6):

$$R_{stack} = \frac{N}{A} \times \left(R_{aem} + R_{cem} + \frac{d_c}{K_c} + \frac{d_c}{K_d} \right) + R_{el} \tag{6}$$

Maximum power density is calculated from Equation 7:

$$P_{max} = \frac{(E_{OCV})^2}{4R_{stack}} \tag{7}$$

Accordingly, gross power density is defined as maximum power density per unit area and calculated from Equation 8:

$$P_{gross} = \frac{P_{max}}{2AN} \tag{8}$$

A is the effective single membrane area (m^2) and N is the number of the membrane cells (dimensionless).

Although commercial ion exchange membranes have been used in most of the published research on RED, in recent years, there have been rising publications on tailor-made ion exchange membranes. Güler et al. [17] first reported environmentally friendly tailor-made ion exchange membranes for RED applications using polyepichlorohydrin (PECH) and 1,4-diazabicyclo-[2.2.2.]octane (DABCO). The thickness of AEMs was around 33 µm with low area resistance (0.82 Ωcm^2) and high power density of 1.27 W/m^2. The CEMs were manufactured from sulfonated polyetheretherketone (SPEEK) [9]. Lopez et al. [22] prepared both AEMs and CEMs using poly(epichlorohydrin) and polyvinyl chloride and modified with chemical agents for laboratory-scale RED stack. The properties of their AEMs and the reference AEMs were similar [17]. CD$_{fix}$ and consequently permselectivity were observed to be slightly higher. After modification with polyethyleneimine, the membrane properties were observed as similar to the Fujifilm Type 10 commercial membrane [23]. In that work, by comparing both synthesized and commercial CEMs, IEC of the membranes was found to be similar, but SD was slightly higher. For the modified CEMs, the IEC, CDfix and permselectivity values were found to be lower than the commercial Fujifilm Type 10 CEM because commercial membranes were profiled and this profile keep the intermembrane gap in the section of feed [23-26].

In order to improve ion selectivity in IEMs, surface modification technique is used. They are divided into four groups which are highly crosslinked layer, layer by layer (LBL) film, oppositely charged layer, dense and neutral layer. Novel bulk morphology, blending of polymers, organic and inorganic hybrid IEMs and different ion exchange groups can be used to control the ion selectivity [27]. Liu et al. [28] prepared surface modified AEMs to have monovalent anion selectivity by infiltration and photo crosslinking technique. Optimum membrane exhibited the highest permselectivity of 11.21 for achieving monovalent anion selectivity that remains constant and this value is higher than the commercial SelemionVR ASV membrane and the other monovalent anion selective membranes published in the literature. Liu et al. [29] used layer by layer deposition method to acquire monovalent selectivity. In this study, polyelectrolyte multilayers added to the commercial AEMs and the permselectivity value of the optimum membrane was increased from 0.39 to 4.36.

3. Types of IEMs in RED system

The IEMs are the essential parts for the RED system because the membrane properties and production of salinity gradient energy are directly proportional to each other. CEMs and AEMs are used in the RED system. AEMs have positively charged fixed groups, in contrast, CEMs have negatively charged groups [30]. Cation and anion exchange groups are shown in Table 1.

In accordance with their manufacturing processes and spatial layout, IEMs can be categorized as homogeneous and heterogeneous [31].

Membrane heterogeneity is an important factor for characterization of the ion exchange membranes especially for determining the water uptake (WU). It represents the fraction of empty space in a membrane matrix that is filled with a solution or electrolyte. Heterogeneous IEMs have a greater inter gel phase than homogeneous IEMs as seen in Figure 3. As a result, the permselectivity of membrane and counter-ion transport number will be reduced. IEC is a parameter that the number of functional sites in a membrane matrix. The concentration of functional sites in the membrane is critical for achieving a higher selectivity. The ratio of IEC to WU will define the effect of Donnan exclusion.

3.1. Nanocomposite IEMs

Nanocomposite IEMs are modified version of conventional polymeric membranes and they are prepared through incorporation of organic and inorganic nanoparticles (NPs) into the polymeric membranes. Nanocomposite membranes are divided into two groups as thin film and mixed matrix (Figure 4). Blending of nanoparticles with polymer solution, in-situ polymerization, melt-mixing, in-situ sol-gel and dipping are the methods available for the incorporation of nanomaterials into ion exchange membranes [33,34]. Among them, the most common technique used in the production of polymeric nanocomposite IEMs is solution blending. In this method, the polymer is first dissolved in a solvent, and then nanoparticles are added into the polymeric solution. Homogeneous distribution of nanoparticles within the polymer is achieved by sonication or mixing. The solvent is then evaporated and the nanoparticles are incorporated in the polymer [33]. It is a simple method and has the advantage of being easily reproducible, so it is suitable for large scale production.

In-situ polymerization method uses monomers instead of polymers, similar to the solution blending method. The melt-mixing process is solvent-free. The in-situ sol-gel technique involves mixing a polymer with a nanoparticle precursor such as tetraethoxysilane for silica (TEOS) and titanium dioxide. Sol-gel is more costly and time-consuming than the solution blending technique, since it includes hydrolysis and polycondensation stages [33].

The described papers present the effect of titania nanoparticles on various filtration mostly. Vatanpour et al. [35] produced a TiO_2-trapped mixed matrix membrane by blending the nanoparticles with casting solution by phase inversion and the fouling resistance of the membranes were examined. They found that the flux recovery was increased by mixing 4 wt % of TiO_2 nanoparticles and at low quantities of TiO_2, the relatively small size nanoparticles led to increased reduction of biofouling. In another study, polyethersulfone (PES) / poly (vinyl alcohol) (PVA) / TiO_2 composite nanofiltration (NF) membranes were prepared by dipping the membrane into aqueous solutions of TiO_2 nanoparticles, and glutaraldehyde (GA) was used as a crosslinker to increase stability and the thermal, chemical and mechanical properties of membranes [36]. Madaeni and Ghaemi [37] investigated the characterization of anti-fouling self-cleaning RO membranes coated with TiO_2 particles by the method of dipping in nanoparticle solution. Damodar et al. [38] studied the fouling resistance, antibacterial and photocatalytic properties of polyvinylidene fluoride (PVDF) membranes prepared by adding different amounts of TiO_2 particles (0-4% by weight) to the casting solution.

Nano materials used in ion exchange membranes are silica, copper, silver, titanium dioxide, iron (II, III) oxide, zinc oxide, zeolite, graphene and carbon nanotube [33]. Silver nanoparticles have antimicrobial properties due to their small size, large surface area and ability to attach to matrices. Various nanoparticles such as zinc, titanium, copper, alginate, gold have been used to provide antimicrobial properties, but silver is the most effective nanoparticle against viruses, bacteria and other eukaryotes [39]. In addition to its antimicrobial properties, an improvement was observed in selective permeability, ionic flux, ionic conductivity, thermal stability and membrane potential values compared to the unmodified membrane when anion-exchange membranes were coated with silver nanoparticles [33]. Silver nanoparticles are produced either by synthesizing first and then adding it to the casting solution as an organic suspension, or by in situ reductions of ionic silver by the polymer-solvent.

For less porous membranes, the effects of filler addition are more pronounced. This provides an improvement in separation properties with only a small reduction in rejection and a significant reduction in hydraulic resistance [39]. For casting mixtures giving membranes of relatively low porosity, there is macro-void expansion and an increase in surface pore size and density. To control the agglomeration and distribution of nanoparticles, limiting agents and ionic strength control are often used. Many synthetic and natural polymers such as polyvinylpyrrolidone (PVP), polyvinyl alcohol (PVA), polyacrylates, polyacrylamide, dextrin and casein are used as silver nanoparticle stabilizers [40].

Li et al. [41] prepared PVDF membranes modified with polyacrylic acid (PAA) grafted silver nanoparticles in three steps. Firstly, the membrane was

prepared by phase inversion method, in the second stage, polyacrylic acid grafting was carried out by wetting the membrane surface with azo-bis-isobutylnitrile (AIBN) and immersion in acrylic acid solution and the fouling resistance of the membranes was studied. Lee et al. [42] investigated the fouling resistance of thin film polyamide composite membranes on which silver nanoparticles were fixed by polymer blending technique. In another study, silver nanoparticles were added to thin film composite membranes by blending with a polymer casting solution to prevent biological contamination and contamination resistance was investigated [43]. Uz et al. [44] worked on the development of antibacterial polyacrylonitrile membranes trapped with $AgCl-TiO_2$ xerogels. The membrane is produced by the phase inversion, the nanoparticles are added to the membrane by blending with the polymer casting solution and the fouling resistance was examined.

The first study on nanocomposite ion exchange membranes for RED applications was reported on CEMs [45]. In that study, functionalized iron (III) oxide ($Fe_2O_3-SO_4^{2-}$) was taken as inorganic filler. Custom-made nanocomposite membrane was equated with commercial membrane in terms of power generation performance. Tong et al. [46] studied nanocomposite CEMs made of oxidized multi-walled carbon nanotube (o-MWCNT) and they reported that the membrane properties were improved greatly [46].

So far, there is no specific production of nanocomposite anion-exchange membranes for RED applications. Only a limited number of nanoparticles and polymeric materials have been used to synthesize ion exchange membranes, particularly for the RED system. Generally, commercial AEMs were used in the RED studies. Their surfaces were coated with a polyelectrolyte solution to prepare an anti-fouling membrane for ED and RED systems, and thus the ionic resistance of the membranes was reduced and their selective permeability was increased [47-49]. An adequate quantity of effort will likely be dedicated to the advancement of effective energy storage via nanocomposite membranes in the near future [50].

Table 1
Typical cation and anion exchange groups in IEMs [30].

Cation exchange groups	Anion exchange groups
-CF_2SO_3H	$N(CH_3)_3OH$
-SO_3H	-$N(CH_2OH)(CH_3)_2OH$
-CF_2COOH	- $S(CH_3)_2OH$
-COOH	-$P(CH_3)_3$ OH
-PO_3H_2	-NH_2
-Phenolic OH	-NH
- $C(CF_3)_3OH$	-Aniline (NH_2)
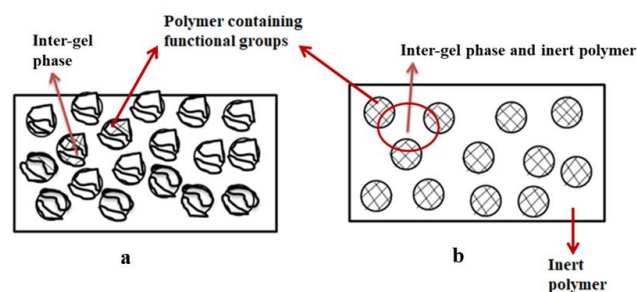
Fig. 3. Structures of the a) homogeneous and b) heterogenous IEMs. (Adapted from [32]).
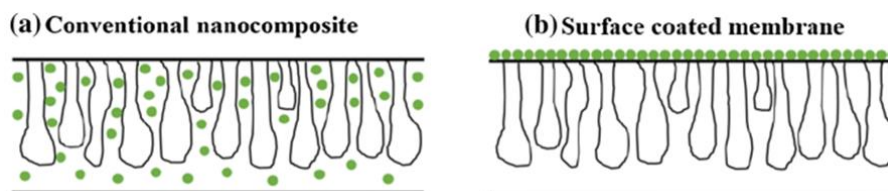
Fig. 4. Representative structures of a) conventional nanocomposite membranes, b) surface coated membranes.

3.2. Pore filling membranes

Pore filling membranes (PFMs) can be prepared by filling ionomers into a porous polymer substrate. The PFMs synthesized with the addition of ionomer or polyelectrolyte have become extremely important in industrial applications of electrochemical energy conversion and storage technologies such as RED [45,51], fuel cells [52-55], and capacitive deionization [56,57].

Haq et al. [56] synthesized PFMs in a porous polyethylene supporting membrane for membrane capacitive deionization and found higher ion exchange capacity (3 meq/g), lower thickness (29 μm) and lower electrical resistance (0.30 Ω·cm^2) than commercial Neosepta AEM membrane. Kim et al. [57] effectively developed pore-filled CEMs with enhanced selectivity for multivalent cations and superior electrochemical characteristics for membrane capacitive deionization.

First pore filling IEMs have been proposed by Yamaguchi et al. [58] for a methanol direct fuel cell. The general requirements such as high ionic conductivity and selectivity are essential for fuel cell and RED processes [59]. For this reason, PFMs have also been tested in a RED system.

A low level of electrical resistance and a high degree of permselectivity are necessary features for IEMs in RED applications [60] and they are fundamental properties that prevail the efficiency of electrical energy conversion [61]. Good mechanical strength and high ionic conductivity are other important properties for the RED system. As shown in Figure 5, these features are achieved using pore filling IEMs composed of a porous substrate and an electrolyte polymer [61,62].

Over the past decade, some studies have examined the preparation of pore filling IEMs for RED applications and studies on this subject are in progress. Pore filling membrane studies on fuel cells applications in the field of electrochemical energy are more common in the literature. Some studies about PFMs in fuel cells are summarized in Table 2.

As shown in Table 2, for PFMs in the fuel cell applications, some porous substrates involved are PAN, CLPE, PP, PES, PI and PE. The pores are usually generated through the introduction of polymer electrolytes in the porous substrates. The easiest way to accomplish this is to pour the ionomers on the membrane surface. When the volatile solvents are totally vaporized, electrolytes flow into channels and an ion exchange membranes can be formed [69]. For the production of PFMs in fuel cells, different techniques were used. Li et al. [68] used plasma to produce composite membranes and excellent performance values were achieved. Jung et al. [52] prepared solid alkaline fuel cell membranes with the solution casting technique and showed that there was deep confinement of methanol and ammonia permeation during this period. Agarwal et al. [68] used an in-situ photopolymerization technique for preparing pore filling Donnan dialysis membrane to separate Au (III) from electronic waste solutions and 96.3% of the initial amount of Au (III) in the feed solution was removed from it. Wang et al. [64] prepared an environmentally friendly pore filling membrane using an in-situ redox graft polymerization technique and PMAA implanted successfully onto PES membrane. The PFMs are fabricated and characterized for direct methanol fuel cells (DMFC) with photopolymerization technique by Kuzume et al. [67] and the power efficiency tests showed that the power density was doubled in comparison with Nafion 112 commercial membrane. Hwang et al. [54] prepared anion exchange PFMs for solid alkaline fuel cells with radio chemical grafting technique and they found that membranes gave a good electrochemical performance with the maximum power and current density values of 127 mW cm^{-2} and 174 mA cm^{-2}.

The PFMs to be used in RED applications should have low DS, high IEC and low electrical resistance. Some detailes about the applications of PFMs in RED tests are explained in Table 3.

Lee et al. [70] prepared the anion conducting PFMs based on quaternized poly(styrene-co-ethylene glycol dimethacrylate) with different monomer: crosslinker weight ratios (1:1; 2:1; 3:1; 4:1; 9:1; 12:1; 16:1). Weight ratio of 4:1 membrane showed the highest maximum power density at 1.5 A m^{-2} and highest mechanical strength (125.8 MPa) due to the highest transport number and lowest water content which are close to the commercial AEM properties. In that study, much lower area resistance, higher IEC and DS were obtained than the commercial Neosepta AMX membranes (ASTOM, Japan). Kim et al. [61] developed one type of anion exchange membrane (KIERAEM1, inner membrane) and two type of cation exchange membranes (KIERCEM1, inner membrane and KIERCEM2, shielding membrane). These membranes showed low area resistances compared to the commercial AEMs and CEMs with the open spacer area of 81.3%. Low area resistances yielded a high gross power density with the value of 2.4 W m^{-2}. Lee et al. [71] prepared thin PFMs for

high power density in RED and they observed effects of membrane structure on resistance, stability and ion selectivity. The prepared membranes carried out a gross power density of 2.43 W m^{-2} which is 1.3-1.8 times higher than three commercial membranes. Choi et al. [74] studied on preparation of anion exchange PFMs.

Kim et al. [57] fabricated thin film composite pore filling IEMs and evaluated them in the RED system with Nernst Planck analysis and model results were verified by testing 100 cell pairs of the single RED stack on a variety of parameters including voltage, current, and power. The modified Nernst Planck equation was proven to be valid for both commercial membranes and the heterogeneous thin composite PFMs.

Yang et al. [73] prepared pore filling CEMs (PFCEMs) with roll to roll fabrication using porous polyethylene supporter with green fabrication method and applied it in reverse electrodialysis. The IEC, permselectivity, and area resistance of these membranes were 1.80 mequiv g^{-1}, 95.7%, and 0.42 Ω cm^2, respectively, which are close to those of commercial membranes and they also exhibited higher power density of 1.95 W m^{-2} in comparison to commercial membranes (1.46 Wm^{-2}). Choi et al. [74] studied on fabrication of thin film PFMs with non-conductive materials and found the highest gross and net power density as 1.39 W m^{-2} and 0.90 W m^{-2}, respectively, with 10 cell pairs.
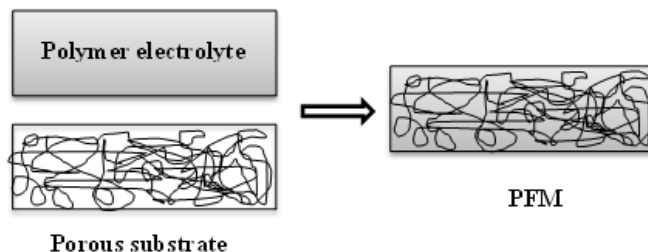

Fig. 5. The preparation of the PFM (Adapted from [63]).

Table 2
Porous substrates, polymer electrolytes and techniques used for PFMs in the fuel cell applications.

Porous substrate	Polymer electrolyte	Technique	Reference
Poly(ether sulfone) (PES)	Polymethylacrylic acid (PMAA)	Redox-graft polymerization	[64]
Crosslinked polyethylene (CLPE)	Amminated Asahi polysulfone (AM-APS) solution	Solution casting	[65]
Polyacryonitrile (PAN)	Poly(ethylene glycol) methacrylate (PEO526OHMA)	Atmospheric dielectric barrier discharge (DBD) plasma graft filling	[66]
Polyimide (PI)	Poly-2-acrylamide-2-methylpropanesulphonic acid (PAMPS) and polystyrene sulphonic acid (PSS)	Photopolymerization	[67]
Meso-porous polyethylene (PE)	Trimethylamine (TMA)	Radio-chemical grafting	[54]
Polypropylene (PP)	**Spacer**-(3-acryloxypropyl) trimethoxysilane (APTMS), **Crosslinker**-ethylene Glycoldimethacrylate (EGDMA)	In-situ photo polymerization	[68]

Table 3
Properties of PFMs for RED applications mentioned in the literature.

Membrane type	IEC (meq g^{-1})	DS (%)	Thickness (μm)	AR (Ω cm^2)	Permselectivity (%)	Reference
AEM	2.36	37.4	35-40 μm	0.303	-	[70]
CEM1	2.64	26.9	26	0.34	97.8	
AEM	1.55	21.9	27	0.28	91.8	[61]
CEM2	1.42	21.7	26	0.72	99.2	
AEMW1-2	1.69	37.9	Dry: 16 Wet:21	0.23	93.4	
CEMW1-1	1.41	29.3	Dry: 16 Wet:19	0.51	99.8	[71]
CEMW1-2	1.61	43.1	Dry: 16 Wet:21	0.35	97.5	
AEM	1.26	21.3	25	0.764	93	[72]
CEM	N.A.	N.A.	16	95.7	42.1	
AEM			16	92.4	40.2	[57]
CEM	1.81	49.5	Dry:16 Wet: 20	0.40	92.4	[73]
AEM	N.A.	N.A.	20	0.46	98.1	
CEM			21	0.32	99	[74]

3.3. Antifouling IEMs

Although there are vast potential of energy generation from mixing seawater and river water using RED, one of the crucial restrictions of using RED process is fouling of IEMs causing some reduction in the net power density produced [3]. Membrane fouling is strongly affected by the source and type of feed solution due to different contaminants available. One of the difficulties associated with operating RED is fouling. Major types of pollutants are colloidal (clays, flocs), organic (oils, polyelectrolytes, humics), scaling (mineral precipitates) and biological (bacteria, fungi) and multivalent ions (such as Mg^{2+}). Scaling is more prone to occur with CEMs in RED system depending on the morphological and electrochemical properties. It has been demonstrated that novel membranes and specialized spacers are effective in limiting scaling [83]. Fouling is another issue that significantly reduces the power density (greater than 50%). Organic fouling depends on the amount of the total organic components in high salinity and low salinity compartments of the RED system. The chemical stability and structural deterioration of IEMs should be analyzed for determining the effect of organic fouling [83].

Fouling reduces process efficiency and raises process cost. It is reported that the anti-organic-fouling properties of the aliphatic anion exchange membranes are better than those of aromatic AEMs. Inorganic scaling takes place when salts in the water precipitate and accumulate on the membrane surface. The major scaling ions are calcium, magnesium, barium, sulphate and bicarbonate [75].

Flow channels and spacers clogging occur because of biofouling. This is a principal threat for this system due to the extra cost and increased energy losses for pumping [3]. Organic and biofouling are the main problems affecting AEMs in the ED system [48,76]. Scaling due to inorganic ions (Ca^{2+}, Mg^{2+}) is common in CEMs [7,72]. Periodic (back) washing techniques were used to prevent and control fouling in RED systems [74].

Solutions for membrane fouling are pre-treatment, operation optimization and chemical cleaning. On the other hand, these solutions may cause some difficulties. These are listed below [78]:

- Ineffective pre-treatment can lead to high rates of contamination.
- No comprehensive consideration on the mechanics of nucleation and scaling.
- Fouling may result in morphological deterioration to the membrane.

Constant loads on the membrane surface affect the type and rate of fouling [19]. It is stated that fouling of AEMs by organic matter (humic acids) is a possible cause that lowers RED performance. Aromatic AEMs have low permselectivity values while only resistance increase was observed with aliphatic AEMs having medium swelling degree. On the other hand, aliphatic AEMs with large swelling degree displayed permselectivity decrease. As a result, fouling of AEMs causes a certain decrease in OCV values and RED performances [79].

The pressure drop will increase with colloidal and biofouling and hence the net power density will decrease [7]. For the practical implementation of RED, one of the most significant challenges is pollution. Fouling enhances resistance and reduces permselectivity. Therefore it can reduce power density by 60%. It is stated that spacers are also important factor in membrane fouling and when compared to membranes they are more sensitive to biofouling [19].

Fouling is more prevalent in AEMs because of the interaction between their negatively and positively charged groups. To control fouling, highly selective AEMs can be developed without increasing the membrane electro-resistance. For this, different surface modification techniques can be applied. These modification techniques can be classified as graft polymerization, dip coating/immersion, electrodeposition, layer by layer deposition, plasma treatments, solution casting [80].

Humic acid absorption, electrochemical impedance spectroscopy (EIS) and fluorescence spectroscopy methods are used for fouling resistance measurement in the RED system. To determine the humic acid sorption of different AEMs, they were left in the humic acid solutions and the absorbed humic acid ratios were measured with uv-vis spectrophotometer. The power density, membrane area resistance, and permeactivity values of the membrane were determined [79]. Pintossi et al. [81] used EIS as a new approach to observe cleaning and fouling in the RED system. To improve fouling and cleaning monitoring, some experiments were performed with sodium dodecyl benzene sulphonate (SDBS), while at the same time EIS was measured at the RED stack level. The pollution property of the RED system caused by the dissolved organic substances in seawater and river water was determined by the fluorescence spectroscopy method. The color changes of AEMs and spacers in contact with river water were more greater than those in contact with seawater [82].

4. Conclusions

Salinity gradient energy (i.e. blue energy) can be directly transformed to electrical power using RED technology. The properties of the ion exchange membranes significantly affect the overall RED performances, particularly power density. Many works have concentrated on customizing the properties of IEMs in recent years to ensure low resistance and high permselectivity. Recently, nanocomposite IEMs and pore-filling IEMs attract the interests of membrane researchers greatly. In addition, preparing antifouling IEMs for RED applications is highly important because fouling increases the membrane resistance and decreases the permselectivity. Although recent advancements of the preparations of the ion exchange membranes and performances were proven at laboratory scale, further pilot-scale investigations are necessary to validate the performances of novel tailored-made IEMs in RED applications.

References

[1] E. Güler, Anion Exchange Membrane Design for Reverse Electrodialysis, PhD Thesis, University of Twente, 2014.

[2] S. Pawlowski, Experimental and Modeling Studies on Reverse Electrodialysis for Sustainable Power Generation, PhD Thesis, Universidade Nova de Lisboa, 2015.

[3] J.W. Post, Blue Energy: Electricity Production From Salinity Gradients by Reverse Electrodialysis, Wageningen University, PhD Thesis, 2009.

[4] J.W. Post, J. Veerman, H.V.M. Hamelers, G. J.W. Euverink, S.J. Metz, K. Nymeijer, C.J.N. Buisman, Salinity-gradient power: Evaluation of pressure-retarded osmosis and reverse electrodialysis, J. Membr. Sci. 288 (2007) 218–230. 10.1016/j.memsci.2006.11.018.

[5] G.Z. Ramon, B.J. Feinberg, E.M.V. Hoek, Membrane-based production of salinity-gradient power., Energy Environ. Sci. 4 (2011) 4423-4434. https://doi.org/10.1039/C1EE01913A.

[6] Q. She, X. Jin, Q. Li, C.Y. Tang, Relating reverse and forward solute diffusion to membrane fouling in osmotically driven membrane processes. Water Res. 46 (7) (2012) 2478-2486. 10.1016/j.watres.2012.02.024.

[7] D.A. Vermaas, D. Kunteng, M. Saakes, K. Nijmeijer, Fouling in reverse electrodialysis under natural conditions. Water Res. 47 (2013) 1289-1298, http://dx.doi.org/10.1016/j.watres.2012.11.053.

[8] M. Tedesco, H. V. M. Hamelers, P. M. Biesheuvel, Nernst-Planck transport theory for (reverse) electrodialysis: I. Effect of co-ion transport through the membranes, J. Membr. Sci. 510 (2016) 370–381. http://dx.doi.org/10.1016/j.memsci.2015.05.020.

[9] E. Güler, R. Elizen, D.A. Vermaas, M. Saakes, K. Nijmeijer, Performance-determining membrane properties in reverse electrodialysis, J. Membr. Sci. 446 (2013) 266-276. http://dx.doi.org/10.1016/j.memsci.2013.06.045.

[10] E. Güler, K. Nijmeijer, Reverse Electrodialysis for Salinity Gradient Power Generation: Challenges and Future Perspectives, J. Membr. Sci. Res. 4 (2018) 108-110. 10.22079/JMSR.2018.86747.1193.

[11] H. Strathmann, L., Giorno, E. Drioli, An Introduction to Membrane Science and Technology, 2nd edition, CNR-Servizio Pubblicazioni, 2006.

[12] B.A. Bolto, M.B. Jackson, Polyamine ion-exchange resins from polyepichlorohydrin: Resins with improved resistance to oxidation, Reactive Polymers, Ion Exchangers, Sorbents, (1984) 209-222.

[13] D. H. Kim, MS. Kang, Preparation and characterizations of ionomer-coated pore-filled ion exchange membranes for reverse electrodialysis, Membr. J. (2016) 43-54,.https://doi.org/10.14579/MEMBRANE_JOURNAL.2016.26.1.43

[14] S.C. Yang, Y.W. Choi, J. Choi, N. Jeong, H. Kim, JY. Nam, H. Jeong, R2R fabrication of pore-filling cation-exchange membranes via one-time impregnation and their application in reverse electrodialysis, ACS Sust. Chem. Eng. (2019). https://doi.org/10.1016/j.memsci.2018.12.034.

[15] H. K. Kim, M. S. Lee, S. Y. Lee, Y. W. Choi, N. J. Jeong, C. S. Kim, High power density of reverse electrodialysis with pore-filling ion exchange membranes and a high open area spacer, J. Mater. Chem. A 3 (2015) 16302-16306, 10.1039/c5ta03571f.

[16] X. Tongwen, Y. Weihua, Fundamental studies of a new series of anion exchange membranes: membrane preparation and characterization, J. Membr. Sci. 190 (2001) 159-166. 10.1016/S0376-7388(01)00434-3.

[17] E. Guler, Y. Zhang, M. Saakes, K. Nijmeijer, Tailor-made anion-exchange membranes for salinity gradient power generation using reverse electrodialysis, ChemSusChem 5 (2012) 2262-2270. 10.1002/cssc.201200298.

[18] G.M. Geise, M.A. Hickner, B.E. Logan, Ionic resistance and permselectivity tradeoffs in anion exchange membranes, ACS Appl. Mater. Interfaces 5 (2013) 10294–10301. 10.1039/c4cp03076a.

[19] Y. Mei, C.Y. Tang, Recent developments and future perspectives of reverse electrodialysis technology: A review, Desalination 425 (2018) 156–174. http://dx.doi.org/10.1016/j.desal.2017.10.021.

[20] J. Gi Hong, Y. Chen, Evaluation of electrochemical properties and reverse electrodialysis performance for porous cation exchange membranes with sulfate functionalized iron oxide, J. Membr. Sci. 473 (2015) 210–217. http://dx.doi.org/10.1016/j.memsci.2015.02.039.

[21] P. Długołęcki, A .Gambier, K. Nijmeijer, M. Wessling, 2009, Practical potential of reverse electrodialysis as process for sustainable energy generation. Environ. Sci. Technol. (2008) 6888-6894. 10.1016/j.memsci.2008.03.037.

[22] L.V. López, D.M. Reyes-Valadez, O.A. González-Vargas, V.A. Suárez-Toriello, J.S. Jaime-Ferrer, Custom-Made Ion Exchange Membranes at Laboratory Scale for Reverse Electrodialysis, Membranes 9 (2019), 145. 10.3390/membranes9110145.

[23] J. Moreno, S. Grasman, R. van Engelen, K. Nijmeijer, Upscaling Reverse Electrodialysis, Environ. Sci. Technol. 52 (2018) 10856–10863. 10.1021/acs.est.8b01886.

[24] S. Hosseini, A. Gholami, S. Madaeni, A. Moghadassi, A. Hamidi, Fabrication of (polyvinylchloride/cellulose acetate) electrodialysis heterogeneous cation exchange membrane: Characterization and performance in desalination process. Desalination

[25] S.M. Hosseini, B. Rahzani, H. Asiani, A.R. Khodabakhshi, A.R. Hamidi, S.S. Madaeni, A.R. Moghadassi, A. Seidypoor, Surface modification of heterogeneous cation exchange membranes by simultaneous using polymerization of (acrylic acid-co-methyl methacrylate): Membrane characterization in desalination process, Desalination 345 (2014) 13–20. https://doi.org/10.1016/j.desal.2014.04.028.

[26] R.A. Tufa, S. Pawlowski, J. Veerman, K. Bouzek, E. Fontananova, G. di Profio, S. Velizarov, J.G. Crespo, K. Nijmeijer, E. Curcio, Progress and prospects in reverse electrodialysis for salinity gradient energy conversion and storage, Appl. Energy 225 (2018) 290–331. https://doi.org/10.1016/j.apenergy.2018.04.111.

[27] T. Luo, S. Abdua, M. Wessling, Selectivity of ion exchange membranes: A review, J. Membr. Sci. 555 (2018) 429–454. https://doi.org/10.1016/j.memsci.2018.03.051.

[28] H. Liu, Y. Jiang, J. Ding, W. Shi, J. Pan, C. Gao, J. Shen, Surface Layer Modification of AEMs by Infiltration and Photo-Cross-Linking to Induce Monovalent Selectivity, AIChE Separations: Materials, Devices and Processes 64 (2018) 993-1000. 10.1002/aic.15975.

[29] H. Liua, H.Ruana, Y. Zhaoa, J. Pana, A. Sottob, C. Gaoa, B. van der Bruggenc, J.Shena, A facile avenue to modify polyelectrolyte multilayers on anion exchange membranes to enhance monovalent selectivity and durability simultaneously, J. Membr. Sci. 543 (2017) 310–318. 10.1016/j.memsci.2017.08.072.

[30] T. Sata, Ion exhange membranes, Preparation, Characterization, Modification and Application, The Royal Society of Chemistry (2004) ,Tokuyama Research, Japan.

[31] J. Jang, Y. Kanga, J.H. Hanb, K. Janga, C.M. Kima, I.S. Kima, Developments and future prospects of reverse electrodialysis for salinity gradient power generation: Influence of ion exchange membranes and electrodes, Desalination 491 (2020) 114540. https://doi.org/10.1016/j.desal.2020.114540.

[32] D. Ariono Khoiruddin, Subagjo, I.G. Wenten, Heterogeneous structure and its effect on properties and electrochemical behavior of ion-exchange membrane, IOP Science, Mater. Res. Express 4 (2017). https://doi.org/10.1088/2053-1591/aa5cd4.

[33] A. Alabi, A. AlHajaj, L. Cseri, G. Szekely, P. Budd, L. Zou, Review of nanomaterials-assisted ion exchange membranes for electromembrane desalination, NPJ Clean Water, 1:10 (2018). 10.1038/s41545-018-0009-7.

[34] J.H. Jhaveri, Z.V.P. Murthy, A comprehensive review on anti-fouling nanocomposite membranes for pressure driven membrane separation processes, Desalination 379 (2016) 137–154. http://dx.doi.org/10.1016/j.desal.2015.11.009.

[35] V. Vatanpour, S.S. Madaeni, A.R. Khataee, E. Salehi, S. Zinadini, H.A., Monfared, TiO₂ embedded mixed matrix PES nanocomposite membranes: influence of different sizes and types of nanoparticles on antifouling and performance, Desalination 292 (2012) 19–29. 10.1016/j.desal.2012.02.006.

[36] S. Pourjafar, A. Rahimpour, M. Jahanshahi, Synthesis and characterization of PVA/PES thin film composite nanofiltration membrane modified with TiO₂ nanoparticles for better performance and surface properties, J. Ind. Eng. Chem. 18 (2012) 1398–1405. 10.1016/j.desal.2012.02.006.

[37] S. Madaeni, N. Ghaemi, Characterization of self-cleaning RO membranes coated with TiO₂ particles under UV irradiation, J. Membr. Sci. 303 (2007) 221–233. 10.1016/j.memsci.2007.07.017.

[38] R.A. Damodar, S.-J. You, H.-H. Chou, Study the self cleaning, antibacterial and photocatalytic properties of TiO₂ entrapped PVDF membranes, J. Hazard. Mater. 172 (2009) 1321–1328. 10.1016/j.jhazmat.2009.07.139.

[39] C.G. Sprick, Functionalization of Silver Nanoparticles on Membranes And Its Influence On Biofouling, MSc. Thesis, University of Kentucky, 2017, https://doi.org/10.13023/ETD.2017.331.

[40] B. Bolto, Z. Xie, Recent Developments in Fouling Minimization of Membranes Modified with Silver Nanoparticles, 2018, J. Membr. Sci. Res. 4 (2018) 111-120. 10.22079/JMSR.2018.79056.1168.

[41] J.-H. Li, X.-S. Shao, Q. Zhou, M.-Z. Li, Q.-Q. Zhang, The double effects of silver nanoparticles on the PVDF membrane: surface hydrophilicity and antifouling performance, Appl. Surf. Sci. 26 (2013) 663–670. http://dx.doi.org/10.1016/j.apsusc.2012.11.072.

[42] S.Y. Lee, H.J. Kim, R. Patel, S.J. Im, J.H. Kim, B.R. Min, Silver nanoparticles immobilized on thin film composite polyamide membrane: characterization, nanofiltration, antifouling properties, Polym. Adv. Technol. 18 (2007) 562–568. 10.1002/pat.918.

[43] J. Yin, Y. Yang, Z. Hua, B. Deng, Attachment of silver nanoparticles (AgNPs) onto thin-film composite (TFC) membranes through covalent bonding to reduce membrane biofouling, J. Membr. Sci. 441 (2013) 73–82. http://dx.doi.org/10.1016/j.memsci.2013.03.060.

[44] M. Uz, F.Y. Mahlicli, E. Seker, S.A. Altinkaya, Development of AgCl-TiO₂ xerogels entrapped antibacterial polyacrylonitrile membranes: The effect of high salinity water on silver release, antibiofouling and antibacterial efficacies, Desalination 492 (2020) 114496. https://doi.org/10.1016/j.desal.2020.114496.

[45] J.G. Hong, Y. Chen, Nanocomposite reverse electrodialysis (RED) ion-exchange membranes for salinity gradient power generation, J. Membr. Sci. 460 (2014) 139–147. http://dx.doi.org/10.1016/j.memsci.2014.02.027.

[46] X. Tong, B. Zhang, Y. Chen, Fouling resistant nanocomposite cation exchange membrane with enhanced power generation for reverse electrodialysis. J. Membr. Sci. 516 (2016) 162–171. http://dx.doi.org/10.1016/j.memsci.2016.05.060.

[47] M. Vaselbehagh, H. Karkhanech, S. Mulyati, R. Takagi, H. Matsuyama, Improved antifouling of anion-exchange membrane by polydopamine coating in electrodialysis process, Desalination 332 (2014) 126–133. http://dx.doi.org/10.1016/j.desal.2013.10.031.

[48] M. Vaselbehagh, H. Karkhanechi, R. Takagi, H. Matsuyama, Biofouling phenomena

on anion exchange membranes under the reverse electrodialysis process. J. Membr. Sci. 530 (2017) 232-239. http://dx.doi.org/10.1016/j.memsci.2017.02.036.

[49] H. Gao, B. Zhang, X. Tong, Y. Chen, Monovalent-anion selective and antifouling polyelectrolytes multilayer anion exchange membrane for reverse electrodialysis, J. Membr. Sci. 567 (2018) 68–75. https://doi.org/10.1016/j.memsci.2018.09.035.

[50] J.G. Hong, H. Gao, L. Gan, X. Tong, C. Xiao, S. Liu, B. Zhang, Y. Chen, Nanocomposite and nanostructured ionexchange membrane in salinity gradient power generation using reverse electrodialysis, Advanced Nanomaterials for Membrane Synthesis and its Applications Micro and Nano Technologies (2019) 295-316. https://doi.org/10.1016/B978-0-12-814503-6.00013-6.

[51] J.G. Hong, Y. Chen, Nanocomposite reverse electrodialysis (RED) ion-exchange membranes for salinity gradient power generation, J. Membr. Sci. 460, (2014) 139–147. http://dx.doi.org/10.1016/j.memsci.2014.02.027.

[52] H. Jung, K. Fujii, T. Tamakia, H. Ohashi, T. Ito, T. Yamaguchi, Low fuel crossover anion exchange pore-filling membrane for solid-state alkaline fuel cells, J. Membr. Sci. 373 (2011) 107–111. 10.1016/j.memsci.2011.02.044.

[53] Kang, H., Lee, M.S., Sim, W.J.,Yang, T.H., Shin, K.H., GunShul, Y., Choi, Y.W., Effect of number of cross-linkable sites on proton conducting, pore-filling membranes, J. Membr. Sci. 460 (2014) 178–184. http://dx.doi.org/10.1016/j.memsci.2014.02.037.

[54] D.S. Hwang, A.S. Tauqir, J.Y. Sohn, Y.C. Noh, C. HoonPark, M.D. Guiver, Y.M. Lee, Anisotropic radio-chemically pore-filled anion exchange membranes for solid alkaline fuelcell (SAFC), J. Membr. Sci. 495 (2015) 206–215. http://dx.doi.org/10.1016/j.memsci.2015.07.067.

[55] J. Fang, M. Lyu, X. Wang, Y. Wu, J. Zhao, Synthesis and performance of novel anion exchange membranes based on imidazolium ionic liquids for alkaline fuel cell applications, J. Power Sour. 284 (2015) 517-523. http://dx.doi.org/10.1016/j.jpowsour.2015.03.065.

[56] Haq, O., Choib, J.H., Lee, Y.S., 2018, Anion-exchange membrane for membrane capacitive deionization prepared via pore-filling polymerization in a porous polyethylene supporting membrane, React. Funct. Polym. 132, 36–42. https://doi.org/10.1016/j.reactfunctpolym.2018.09.010.

[57] H. Kim, N. Jeong, S.C. Yang, J. Choi, M.S. Lee, J.Y. Nam, E. Jwa, B. Kim, K. Ryu, Y.W. Choi,Nernst- Planck analysis of reverse-electrodialysis with the thincomposite pore-filling membranes and its upscaling potential, Water Res. 165 (2019) 114970. https://doi.org/10.1016/j.watres.2019.114970.

[58] T. Yamaguchi, F. Miyata, S. Nakaoa, Pore-filling type polymer electrolyte membranes for a direct methanol fuel cell, J. Membr. Sci. 214 (2003) 283–292. 10.1016/S0376-7388(02)00579-3.

[59] A. B. Yaroslavtsev, I. A. Stenina, D. V. Golubenko, Membrane materials for energy production and storage, Pure Appl. Chem. (2020). https://doi.org/10.1515/pac-2019-1208.

[60] P.Długołecki, K. Nymeijer, S. Metz, M. Wessling, Current status of ion exchange membranes for power generation from salinity gradients, J. Membr. Sci. 319 (2008) 214–222. 10.1016/j.memsci.2008.03.037.

[61] H. K. Kim, M. S. Lee, S. Y., Lee, Y. W. Choi, N. J. Jeong, C. S. Kim, High power density of reverse electrodialysis with pore-filling ion exchange membranes and a high open area spacer, J. Mater. Chem. A 3 (2015) 16302-16306. 10.1039/c5ta03571f.

[62] D.H. Kim, J.S. Park, M. Choun, J. Leeb, M.S. Kang, Pore-filled anion-exchange membranes for electrochemical energY conversion applications, Electrochimica Acta 222 (2016) 212–220. http://dx.doi.org/10.1016/j.electacta.2016.10.041.

[63] Kim D. H., Kang MS., 2016, Preparation and characterizations of ionomer-coated pore-filled ion exchange membranes for reverse electrodialysis, Membr. J. 26, 43-54. https://doi.org/10.14579/MEMBRANE_JOURNAL.2016.26.1.43.

[64] M. Wang, Q.F. Ana, L.G. Wu, J.X. Mob, C.J. Gaoa, Preparation of pH-responsive phenolphthalein poly(ether sulfone) membrane by redox-graft pore-filling polymerization technique, J. Membr. Sci. 287 (2007) 257–263. 10.1016/j.memsci.2006.10.049.

[65] H. Jung, K. Fujii, T. Tamaki, H. Ohashi, T. Ito, T. Yamaguchi, Low fuel crossover anion exchange pore-filling membrane for solid-state alkaline fuel cells, J. Membr. Sci. 373 (2011) 107–111. 10.1016/j.memsci.2011.02.044.

[66] Z. Li, B. Zhang, L. Qu, J. Ren, Y. Li, A novel atmospheric dielectric barrier discharge (DBD) plasma graft-filling technique to fabricate the composite membranes for pervaporation of aromatic/aliphatic hydrocarbons, J. Membr. Sci. 37 (2011) 163–170. 10.1016/j.memsci.2011.01.035.

[67] A. Kuzume, Y.M. MasatokiIto, Characterisation of PAMPS–PSS pore-filling membrane for direct methanol fuelcell, J. Membr. Sci. 446 (2013) 92–98. http://dx.doi.org/10.1016/j.memsci.2013.06.032.

[68] C. Agarwal, J.W. Cattrall, S.D. Kolev, Donnan dialysis based separation of gold(III) from electronic waste solutions using an anion exchange pore-filled membrane, J. Membr. Sci. 514 (2016) 210–216. http://dx.doi.org/10.1016/j.memsci.2016.04.033.

[69] J. Ran, L. Wu, Y. He, Z. Yang, Y. Wang, C. Jiang, L. Ge, E. Bakangura, T. Xu, Ion exchange membranes: New developments and applications, J. Membr. Sci. 522 (2017) 267–291.http://dx.doi.org/10.1016/j.memsci.2016.09.033.

[70] S. Lee, M.S. Shin, J.S. Park, Anion-conducting Pore-filling Membranes with Optimization of Transport Number and Resistance for Reverse Electrodialysis, Chem. Soc. Japan, 43 (2014) 621–623. 10.1246/cl.131221.

[71] M.S. Lee, H.K. Kim, C.S. Kim, H.Y. Suh, K.S. Nahm, Y.W. Choi, Thin Pore-Filled Ion Exchange Membranes for High Power Density in Reverse Electrodialysis: Effects of Structure on Resistance, Stability, and Ion Selectivity, Chem. Select 2 (2017) 1974 – 1978. 10.1002/slct.201700167.

[72] J. Choi, S.C. Yang, N.J. Jeong, H. Kim, W.S. Kim, Fabrication of an Anion-Exchange Membrane by Pore-Filling Using Catechol−1,4-Diazabicyclo-[2,2,2]octane Coating and Its Application to Reverse Electrodialysis, Langmuir, 34 (2018) 10837−10846. 10.1021/acs.langmuir.8b01666.

[73] S.C. Yang, Y.W., Choi, J., J.N. Choi, H. Kim, J.Y. Nam, H. Jeong, R2R fabrication of pore-filling cation-exchange membranes via one-time impregnation and their application in reverse electrodialysis, ACS Sust. Chem. Eng. 7 14 (2019). 12200-12213. 10.1021/acssuschemeng.9b01450.

[74] J. Choi, W.S. Kim, H.K. Kim, S.C. Yang, S.C. Jeong, Ultra-thin pore-filling membranes with mirror-image wave patterns for improved power density and reduced pressure drops in stacks of reverse electrodialysis, J. Membr. Sci. 620 (2021) 118885. https://doi.org/10.1016/j.memsci.2020.118885.

[75] S. Mikhaylin, L. Bazinet, Fouling on ion-exchange membranes: classification, characterization and strategies of prevention and control. Adv. Colloid Interface Sci. 229 (2016) 34-56. 10.1016/j.cis.2015.12.006.

[76] H.J. Lee, M.K. Hong, S.D. Han, S.H. Cho, S.H. Moon, Fouling of an Anion Exchange Membrane in the Electrodialysis, Desalination 238 (2009) 60-69. https://doi.org/10.1016/j.desal.2008.01.036.

[77] J.L. Di Salvo, Cosenza, A., Tamburini, A., Micale, G., Cipollina, A., Long-run operation of a reverse electrodialysis system fed with wastewaters, J. Environ. Manag. 217 (2018) 871-887. https://doi.org/10.1016/j.jenvman.2018.03.110.

[78] L. N. Le, S. P. Nunes, Materials and membrane technologies for water and energy sustainability, Sust. Mater. Technol. 7 (2016) 1–28. https://doi.org/10.1016/j.susmat.2016.02.001.

[79] T. Rijnaarts, J. Moreno, W. Saakes, V.M. Vosb, K. Nijmeijer, Role of anion exchange membrane fouling in reverse electrodialysis using natural feed waters, Colloid. Surf. A 560 (2019) 198–204. https://doi.org/10.1016/j.colsurfa.2018.10.020.

[80] F. Kotoka, I. Merino-Garcia, S. Velizarov, Surface Modifications of Anion Exchange Membranes for an Improved Reverse Electrodialysis Process Performance: A Review, Membranes, 10 (2020) 160. 10.3390/membranes10080160.

[81] D. Pintossi, M. Saakes, Z. Borneman, K. Nijmeijer, Electrochemical impedance spectroscopy of a reverse electrodialysis stack: A new approach to monitoring fouling and cleaning, J. Power Sources 444 (2019) 227302. https://doi.org/10.1016/j.jpowsour.2019.227302.

[82] K. Chon, N. Jeong, H. Rhoc, J-Y. Namb, E. Jwab, J. Chod, Fouling characteristics of dissolved organic matter in fresh water and seawater compartments of reverse electrodialysis under natural water conditions, Desalination (2020) 114478. https://doi.org/10.1016/j.desal.2020.114478.

[83] S. Santoro, R. A. Tufa, A. H. Avc, E. Fontananova, G. D. Profio, E. Curcio, Fouling propensity in reverse electrodialysis operated with hypersaline brine, Energy 228 (2021) 120563. https://doi.org/10.1016/j.energy.2021.120563.